Multiple Sensor Data Association Algorithm Using Hough Transform for Track Initiation

Emil Semerdjiev **Kiril Alexiev** **Ludmil Bojilov**
Bulgarian Academy of Sciences, Central Laboratory for Parallel Processing,
"Acad. G. Bonchev" Str., Bl. 25-A, 1113 Sofia, Bulgaria, E-mail:signal@acad.bg;

Abstract. *This paper is concerned with the problem of associating data from multiple sensors (radars). A new data association approach using Hough transform is proposed for rectilinear track initiation. It is intended to overcome the combinatorial explosion and the synchronisation problems arising in the multitarget multisensor case.*

Keywords: multiple sensor data association, Hough-transform, track initiation

1. Introduction

The data association (DA) problem is of significant importance in the process of building up multiple sensor systems for tracking multiple targets. DA problem can be mathematically formulated as a well studied assignment (or matched) problem. In practical implementation of tracking systems, however, some drawbacks arise, the most important of which is the so-called "combinatorial explosion".

The 2D assignment problem can be easily solved by using any of the existing algorithms. In more general case, when the number of sensors S exceeds two ($S \geq 3$) the corresponding assignment problem is known to be NP-hard. Many works are devoted to overcome this difficulty. They make trade-off with optimality achieving in the same time considerable speed up of algorithm processing [1]. The most general solution of this problem is proposed in [2]. The designed there sub-optimal algorithm provides at any stage an estimation of how close it is to the optimal solution.

Another important drawback concerns the synchronisation of the incoming data. In some works the authors accept that all items in the particular list of data are detected at one and the same time [1] and in another works in the algorithms proposed there are included techniques reducing received data items at one and the same instance of time.

Special attention deserves the case connected with dense target scenario and heavy clutter when most of the known algorithms reduce dramatically their efficiency.

A new multisensor DA approach is presented here using Hough transform (HT). The designed HT algorithm (HTA) overcomes the mentioned above problems. It presumes that S two-dimensional track-while-scan radars observe simultaneously area of common coverage (referred to as *Feature space*, FS). All radar measurements are sent to a common processing centre. By using a specific equation HTA maps each arriving measurement in HT space (referred to as *Parameter space*, PS) and applying particular processing techniques detects the tracks.

In the process of designing the multisensor HTA a few sub-problems are discussed and some solutions are proposed in this paper: an useful equation for measurements transformation from local polar FS co-ordinate system to global PS is proposed (Section 2); a two level discrete structure of PS is proposed and appropriate expressions are derived to connect the radar accuracy with the discretization steps (Section 3 and 4). At last, an expression is proposed to define the track detection threshold (Section 5). Results from a Monte Carlo simulation are given for algorithm efficiency confirmation (Section 6).

2. Hough Transform for Multisensor Track Detection

The HT method is based on the fact that, all points along a straight line positioned in FS can be mapped in a single point in PS [3, 4] (Fig. 1).

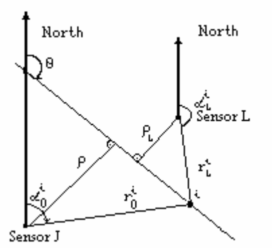

Fig. 1 Sensors and track positions

HTA maps each arbitrarily chosen point from the FS to a curve in the PS. If a set of points in the FS lies along a straight line the corresponding curves are intersected in a single point in the PS. They form a peak of ‘votes’. The key advantage of HT is replacing the difficult problem of feature extraction in the FS by more easy problem of determining of peak location in the PS.

Consider a set of measurements originating from a target moving along straight-line. In the FS, the i-th measurement (r_J^i, α_J^i) (range-azimuth, $r_J^i \in [0, r_J^{\max}]$, $\alpha_J^i \in [0, 360^o])$ arrives in the local polar co-ordinate system $r_J O_J \alpha_J$ of the J-th radar ($J = \overline{1, S}$). In absolute co-ordinate system $rO\alpha$ each sensor has known fixed polar co-ordinates (r_{0J}, α_{0J}) ($r_{0J} \geq 0$, $\alpha_{0J} \in [0, 360^o]$). All co-ordinate systems are oriented to the "North". The earth curvature is neglected.

In this case the local trajectory parameters are (ρ_J, θ) (local trajectory shift - trajectory heading). The respective global parameters are (ρ, θ) (absolute trajectory shift, trajectory heading), where $\theta \in [0, 360^o]$ and $\rho_k \in [0, \rho_{\max}]$. The following equation:

$$\rho = r_J^i \sin(\theta - \alpha_J^i) + r_{0J} \sin(\theta - \alpha_{0J}) \qquad (1)$$

is proposed to map these measurements into the global PS. The first term $\rho_J = r_J^i \sin(\theta - \alpha_J^i)$ maps the measurements from local FS into local PS. The second term shifts them to the global PS.

When the trajectory parameters (ρ, θ) are known and there are no measurement errors, the mapped measurements from all sensors vote in a single point and can be accumulated in a single-point accumulator. After that it is easy to apply some decision rule and to detect the track.

In the real implementation case the parameters (ρ, θ) are unknown. The search is performed in the frame of a fixed discrete set of standard headings $\theta_l = l\,d\theta \in [0, 360^o]$, $l = \overline{0, N_\theta}$ and standard shifts $\rho_m = m\,d\rho \in [0, \rho_{\max}]$, $m = \overline{0, N_\rho}$. Here, $d\theta$ and $d\rho$ are the primary steps of the HTA angular and shift grids, $N_\theta = 360^o / d\theta$ and $N_\rho = \rho_{\max} / d\rho$. By using (1) HTA maps each measurement (r_J^i, α_J^i) from FS in a curve in PS. Consecutively substituting the increasing values of θ_l HTA computes the corresponding shifts $\rho_l^i = \rho(r_J^i, \alpha_J^i, \theta_l)$, $l = \overline{0, N_\theta}$. In this way the single measurement (r_J^i, α_J^i) is mapped in a set of votes lying on curve. If a discrete heading coincides with the real one ($\theta_l = \theta$) the peak of votes (obtained as a result of curves intersection) will locate the shift corresponding to the real trajectory shift (Fig. 2).

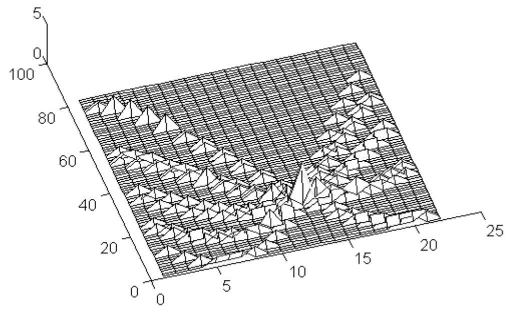

Fig. 2 Peak location

If there is no coincidence between the real and any standard trajectory, or if there are measurement errors, the HTA will detect (with some probability) the standard trajectory with the closest shift and heading instead the real one.

To collect a sufficient number of votes for track detection the mentioned above accumulator point has to be extended to an accumulator area with appropriate sizes $\Delta\rho$ and $\Delta\theta$. This extension of the accumulator sizes both increases the probability of successful measurement voting P_G, and increases the number of the false alarms (FA) voting in it. As a result, the number of the standard trajectories is reduced, diminishing the HTA resolving abilities. The optimal solution is to find the minimal accumulator sizes providing a predefined probability P_G. For this purpose the *pdf*’s of the measurement errors in PS will be identified below.

3. Accumulator Size Definition

In the modern radar systems the sensor’s positioning and orientation errors are negligible.

The measurement errors δr_J^i and $\delta\alpha_J^i$ can be expressed as measurement oscillations around the considered trajectory and the measurements will lie not on a line, but in a strip. We assume a normal distribution for δr_J^i and $\delta\alpha_J^i$ [4], i.e. :

$$\delta r_J^i \sim N(0,\sigma_r^J),\ \delta\alpha_J^i \sim N(0,\sigma_\alpha^J);\ E\left[\delta r_J^i \cdot \delta\alpha_J^i\right]=0,$$

where $E[.]$ is the operator of mathematical expectation and σ_r^J, σ_α^J are the standard deviations of the measurement errors. The sensors can have different accuracy.

The strip defined by the 'maximal' values of these errors has complicated shape depending on the measurement coordinates (Fig. 3).

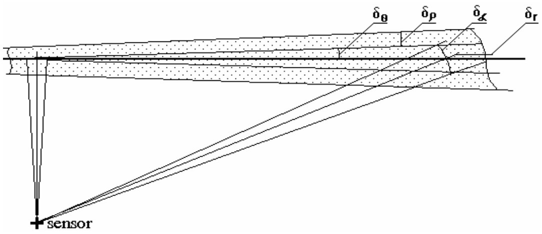

Fig.3 The HTA strip shape

An appropriate experiment (10 000 independent Monte Carlo simulation runs) shows the shapes and the sizes of the real measurement error distributions around a fixed known trajectory (Figs. 4-6) for radars with $r^{\max}=100\,km$.

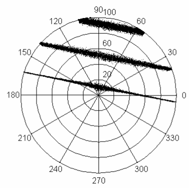

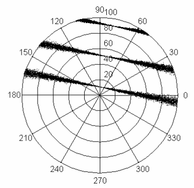

Fig.4 $\sigma_r = 2\,km, \sigma_\alpha = 0^o$. Fig.5 $\sigma_r = 0, \sigma_\alpha = 1.5^o$.

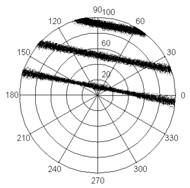

Fig. 6 $\sigma_r = 2\,km, \sigma_\alpha = 1.5^o$.

<u>Single sensor case</u>

We assume that there exists a standard HTA trajectory completely coinciding with that one we observe $\left(\rho_L^J=\rho, \theta_L=\theta\right)$ and respective HTA accumulator (with sizes $\Delta\rho$, $\Delta\theta$) is positioned in the J-th local PS at the point (ρ_L^J, θ_L). The oscillations δr_J^i and $\delta\alpha_J^i$ in FS cause oscillations $\delta\rho_J^i$ and $\delta\theta^i_J$ in the PS.

The first term of the equation (1) and its inverse form: $\theta=\alpha_J^i+\arcsin\left(\rho_J / r_J^i\right)$ are extended in Taylor series up to first-order terms around the standard trajectory. The errors of interest can be expressed as:

$$\delta\rho_J^i=\delta\rho_J^i\left(\delta r_J^i\right)+\delta\rho_J^i\left(\delta\alpha_J^i\right),$$
$$\delta\rho_J^i\left(\delta\alpha_J^i\right)=-\delta\alpha_J^i\, r_J^i \cos(\theta-\alpha_J^i),$$
$$\delta\rho_J^i\left(\delta r_J^i\right)=\delta r_J^i \sin(\theta-\alpha_J^i);$$
$$\delta\theta^i_J=\delta\theta^i_J\left(\delta r_J^i\right)+\delta\theta^i_J\left(\delta\alpha_J^i\right),$$
$$\delta\theta_J^i\left(\delta\alpha_J^i\right)=\delta\alpha_J^i,$$
$$\delta\theta_J^i\left(\delta r_J^i\right)=-\frac{\delta r_J^i}{r_J^i}tg(\theta-\alpha_J^i).$$

The angular oscillations, caused by the error $\delta\theta\left(\delta r_J^i\right)$ is due to its behaviour close to the limits $(\theta-\alpha_J^i)\to\pm 0.5\pi$: $\lim\limits_{(\theta-\alpha_J^i)\to\pm 0.5\pi}\left\{\delta\theta\left(\delta r_J^i\right)\right\}=\pm\infty$. To cover such oscillations it is necessary to set the angular accumulator size $\Delta\theta=\pi$. Therefore this error is ignored while choose $\Delta\theta$. The resulting error $\delta\theta^i_J$ becomes *measurement independent*:

$$\delta\theta^i_J \approx \delta\alpha_J^i \sim N\left(0,\sigma_\alpha^J\right).$$

The unavoidable drawback of this simplification is the measurements interchange between accumulators with equal shifts and neighbouring headings .

Another important feature of the considered errors is the measurement dependence of the error $\delta\rho_J^i$. It is a sum of two independent errors with Gaussian *pdf*'s. The first one $\delta\rho_J^i\left(\delta\alpha_J^i\right)$ directly depends on the range $r_J^i \le r_J^{\max}$. The errors $\delta\rho_J^i\left(\delta r_J^i\right)$ and $\delta\rho_J^i\left(\delta\alpha_J^i\right)$ depend on the relative measurement angular position when $(\theta-\alpha_J^i)\to\pm 0.5\pi$.

Consider a strip with a shape similar to that one presented in Fig. 3. Such complicated shape is near-optimal in the considered single sensor case: it requires minimal surface to cover the area of measurement oscillations, when the desired probability P_G is fixed beforehand. In this way it prevents the redundant increasing of the FA number in the strip and also undesired reduction of the HTA resolving abilities. Such a strip can be constructed as a sum of two sub-strips. The first sub-strip approximates the strip shape of the error δr_J^i. It is set with constant width $\delta r_J^{\max} = k\sigma_r^J$ and its shape is rectangular. The size and shape of the second sub-strip concerns the error $\delta\alpha_J^i$ and it is approximated by a sub-strip with the same shape and the 'maximal' size of $\delta\alpha_J^{\max} = k\sigma_\alpha^J$.

The respective accumulator sizes are $\Delta\rho_J = \Delta\rho_J\left(r_J^i, \theta - \alpha_J^i, k\sigma_r^J, k\sigma_\alpha^J\right)$, and $\Delta\theta_J = \Delta\theta_J\left(k\sigma_\alpha^J\right)$. The event that 'measurement votes in this strip' is a sum of two independent events: '$\left|\delta r_J^i\right| \le k\sigma_r^J$' and '$\left|\delta\alpha_J^i\right| \le k\sigma_\alpha^J$'. The probabilities $P_{G^*}^J$, $P_G^{\rho_J}$, and $P_{G^*}^{\theta_J}$ corresponding to these events are connected by the relation:

$$P_{G^*}^J \ge P_{G^*}^{\rho_J} P_G^{\theta_J} = P\left\{\left|\delta r_J^i\right| \le k\sigma_r^J\right\} P\left\{\left|\delta\alpha_J^i\right| \le k\sigma_\alpha^J\right\} = 4\Phi_0^2(k).$$

The dimensions of every strip with complicated shape concerning the trajectory with parameters (ρ, θ) depend on the size $(\Delta\rho, \Delta\theta)$ of corresponding accumulator. The strip with complicated shape can be represented as sum of n rectangular strips corresponding to sub-accumulators $(\theta_i, \rho_j), i = \overline{i_1, i_n}$ with size $(\Delta\rho, \delta\theta)$, if $\Delta\theta = n\delta\theta$. Let consider a trajectory (ρ, θ) in the radar surveillance volume. In this case the parameters of the nearest accumulator can be defined as: $\theta_{i_1} = \delta\theta\, round\left[\left(\theta - 0.5\Delta\theta\right)/\delta\theta\right]$; $\theta_{i_k} = \theta_{i_1} + (k-1)\delta\theta$; $\rho_j = \delta\rho\, round\left(\rho/\delta\rho\right)$.

Another possible strip shape can be obtained through rough rectangular strip shape approximation. Constant accumulator sizes $\Delta\rho_J$ and $\Delta\theta_J$ will correspond to such strip shape. For providing successful vote of measurements arriving from far ranges, the error $\delta\rho_J^i\left(\delta\alpha_J^i\right)$ is approximated by the equation:

$$\delta\rho_J^{\max} \approx \delta\rho_J^i\,(r_J^{\max}) \ge r_J^{\max}\delta\alpha_J^i + \delta r_J^i.$$

The 'new' error is a sum of two independent errors with Gaussian *pdf*'s, but it is *measurement independent*, so the accumulator sizes can be chosen constant: $\Delta\rho_J = \Delta\rho_J\left(r_J^{\max}, k\sigma_r^J, k_\alpha\sigma_\alpha^J\right)$ and $\Delta\theta_J = \Delta\theta_J\left(k_\alpha\sigma_\alpha^J\right)$. This new strip contains the 'optimal' one (in the worst case, when $\rho = 0$, its surface can be twice greater) and will respectively accumulate greater number of FA.

The probability P_G, can be expressed as:

$$P_G = P_G^{\rho_J} P_G^{\theta_J} > 4\Phi_0^2(k), \qquad \text{where}$$

$$P_G^{\rho_J} = P\left\{|\delta r_J^i| \le \Delta\rho - r_J^{\max} k\sigma_\alpha^J,\ |\delta\alpha_J^i| \le k\sigma_\alpha^J\right\} > 2\Phi_0(k).$$

Multisensor case

If set $k = 3$ and chose $\sigma_r = \max_{J=1,S}\left\{\sigma_r^J\right\}$, $\sigma_\alpha = \max_{J=1,S}\left\{\sigma_\alpha^J\right\}$ and $r_{\max} = \max_{J=1,S}\left\{r_J^{\max}\right\}$, all accumulators (and all FS strips) will have equal sizes: $\Delta\theta_J = \Delta\theta = const$ and $\Delta\rho_J = \Delta\rho = const$. Finally, it will be guaranteed that each measurement will vote in the accumulator with following nearly equal high probabilities:

$$P_G \ge P_G^J \ge 4\Phi_o^2(3) > 0.994.$$

In the process of transformation from the local sensor's PS to the common PS the accumulators corresponding to one and the same trajectory have to be matched. This can be done exactly for only these sensor's sub-accumulators, which parameters coincide with the parameters of accumulators and are equal to $\theta_{i_m} = \delta\theta\, round\left(\theta/\delta\theta\right)$. For other sub-accumulators the matching is not exact. As a result the probability P_G reduces insignificantly.

4. Parameter Space Grid Definition

Let a coarse global accumulator grid, with constant steps $\Delta\rho$ and $\Delta\theta$ is defined in the PS and let consider trajectory with arbitrary chosen, unknown parameters (ρ, θ). Consecutively positioning an accumulator with considered above sizes on each of the grid nodes, the closest accumulator position (positions) can be found. The worst case is when the trajectory shift and heading lie exactly on the border between neighbouring standard headings and shifts. Obviously an accumulator overlapping has to be applied to provide fixed probability P_G.

To provide a high probability P_G a global fine grid, with grid steps $d\rho = \left|\rho_l - \rho_{l+1}\right| < \Delta\rho$ and $d\theta = \left|\theta_n - \theta_{n+1}\right| < \Delta\theta$ ($l \in [1, l_{\max}]$ and $n \in [1, n_{\max}]$) is introduced. The closest accumulator's position

(ρ_{cl},θ_{cl}) to the real trajectory position (ρ_J,θ) satisfies the inequalities:

$$0 \le |\rho_{cl} - \rho| = \min_{l \in [1, l_{\max}]} (|\rho_l - \rho|) \le 0.5 d\rho < \Delta\rho ,$$

$$0 \le |\theta_{cl} - \theta| = \min_{n \in [1, n_{\max}]} (|\theta_l - \theta|) \le 0.5 d\theta < \Delta\theta .$$

The obtained minimal probabilities P_G are:

$$P_G > P_G^{\rho}\left(\frac{d\rho}{2\sigma_r}\right) P_G^{\theta}\left(\frac{d\theta}{2\sigma_\alpha}\right),$$

$$P_G^{\rho}\left(\frac{d\rho}{2\sigma_r}\right) \ge \Phi_0\left(3 - \frac{d\rho}{2\sigma_r}\right) + \Phi_0\left(3 + \frac{d\rho}{2\sigma_r}\right),$$

$$P_G^{\theta}\left(\frac{d\theta}{2\sigma_\alpha}\right) = \Phi_0\left(3 - \frac{d\theta}{2\sigma_\alpha}\right) + \Phi_0\left(3 + \frac{d\theta}{2\sigma_\alpha}\right).$$

It has to be noted that the smaller grid steps increase the probability P_G (see Fig. 4 bellow), but increase the computational load, too.

5. Detection Threshold Definition

Let us introduce the probabilities P_{RTD}^J and P_{FTD}^J for the J-th sensor. The probability $P_{RTD}^J(M_J, N_J)$ is determined as *probability that exactly M_J measurements will be obtained in a fixed number of consecutive complete scans N_J*:

$$P_{RTD}^J(M_J, N_J) = \binom{N_J}{M_J} \left(P_G P_D^J\right)^{M_J} \left(1 - P_G P_D^J\right)^{N_J - M_J} .$$

The probability $P_{FTD}^J(M_J, N_J)$ is determined as *probability to obtain at least one FA per scan in the considered strip in exactly M_J complete scans from N_J consecutive complete scans*:

$$P_{FTD}^J(M_J, N_J) = \binom{N_J}{M_J}\left[1 - \left(1 - P_{fa}^J\right)^{\mu_J}\right]^{M_J} \left(1 - P_{fa}^J\right)^{\mu_J (N_J - M_J)},$$

where the probabilities $P_D^J \ne P_D^M$ and $P_{fa}^J \ne P_{fa}^M$ (if $M \ne J$) are considered as constants and where $\mu_J = \mu_J(\rho, \theta, \Delta\rho)$ is the number of elementary volumes in the considered strip.

In the multisensor case, the probability of true track detection P_{RTD} is determined as *probability that $2 \le M \le N$ measurements will be obtained in $2 \le N = \sum_{J=1}^{S} N_J$ consecutive complete scans in a strip with fixed sizes*:

$$P_{RTD} = \prod_{J=1}^{S} \sum_{i_J = 0}^{N_J} v_{i_J} P_{RTD}^J (i_J, N_J) ,$$

where $v_{i_J} = 1$, if $\sum_{J=1}^{S} i_J \ge M$ and $v_{i_J} = 0$, in the opposite case.

The probability of false track detection P_{FTD} is determined as *probability to obtain at least one FA per scan in $M \ge 2$ complete scans from $N \ge 2$ consecutive complete scans in the considered strip*:

$$P_{FTD} = \prod_{J=1}^{S} \sum_{i_J = 0}^{N_J} v_{i_J} P_{FTD}^J (i_J, N_J) .$$

These probabilities do not take into account the measurements signal parameters.

The sensors can have different sampling intervals T_J. The contributed number of scans N_J by each sensor can be defined just after the common number of scan N is obtained.

By using the Neyman-Pearson criterion, the optimal threshold providing maximal probability P_{RTD} for fixed P_{FTD} can be found in real time.

Additional DA and fusion procedures can be performed upon the measurements from each detected track. Velocity identification and filtering can reject the remaining FA in the single target case. Target state estimation and tracking can be done by Kalman filtering with variable sampling interval. The Multiple hypotheses tracking algorithm [4] can resolve and track the trajectories in the multiple target case.

6. Simulation results

The following scenario has been chosen to estimate algorithm performance: Two radars observe a common target with arbitrary chosen trajectory. Averaging 5000 independent Monte Carlo simulation runs, the next results have been obtained for PS grid sizes: $d\rho = \frac{\Delta\rho}{j}$, $d\theta = \frac{2\Delta\theta}{j}$ ($j = \overline{2,9}$) and radar parameters:

- $r_1 = 70\,km$, $\alpha_1 = 90^o$; $r_1^{\max} = 85\,km$; $\sigma_r^1 = 500\,m$, $\sigma_\alpha^1 = 0.5^o$, $T_1 = 3\,s$;
- $r_2 = r_1$, $\alpha_2 = 0^o$, $r_2^{\max} = r_1^{\max}$, $\sigma_r^2 = \sigma_r^1$, $\sigma_\alpha^2 = \sigma_\alpha^1$, $T_1 = T_2$;
- $P_D^J = 1$ and $P_{FA}^J = 0$.

In addition the sub-accumulator size is assumed equal to PS grid step.

Fig. 7 illustrates the dependence of P_G on strip width and on (accumulator size)/(grid step size) ratio. The curves in this figure are grouped subject to strip width. The solid lines in any group express particular sensor's probabilities P_G depending on number of sub-accumulators in the strip (i.e. accumulator size/grid step size ratio).

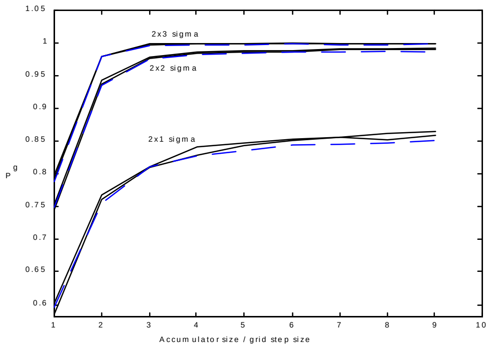

Fig. 7 Dependence of the probability P_G on the accumulator and parameter grid steps sizes.

As it can be seen on the figure the multisensor case (the dashed lines) P_G is slightly worse. This case, however, ensures optimal choice of detection threshold, as it is illustrated in Fig. 8 and 9. In Fig. 8 P_{FTD} and P_{RTD} are given subject to number of obtained measurements for four different sensors ($P_D^1 = 0.3$, $P_{FA}^1 = 5\times10^{-5}$; $P_D^2 = 0.5$, $P_{FA}^2 = 10^{-5}$; $P_D^3 = 0.8$, $P_{FA}^3 = 5\times10^{-6}$; $P_D^4 = 0.9$, $P_{FA}^4 = 10^{-6}$).

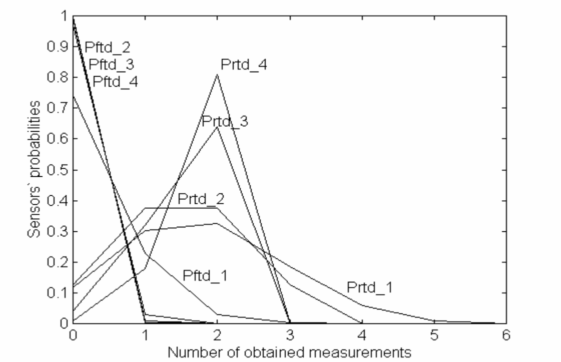

Fig. 8. *Pdf*'s of the events of a real and of a false track multisensor detection

After data fusion (multisensor case, Fig. 9) the disposition of curves of fused P_{FTD} and P_{RTD} allows the optimal choice of detection threshold.

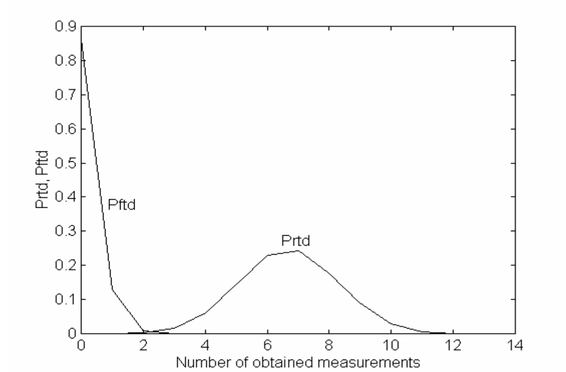

Fig. 9. *Pdf*'s of the events of a real and of a false track single-sensor detection

7. Conclusions

Multiple-sensor data association algorithm for rectilinear tracks initiation is proposed in the paper. It uses the modified Hough transform algorithm to assign the measurements arriving from multiple sensors to a fixed set of standard straight-line trajectories and to reject the false alarms. The measurements arrive without any synchronisation, with different accuracy and have different probabilities for real and false target detection. A relationship for measurements transformation from polar FS co-ordinate system to PS is proposed. The equations for the accumulator sizes, for the grid steps and for the track detection threshold are derived.

The proposed algorithm has increased false alarm resistance and requires a short time for track initiation.

8. References

[1] Deb S., K. Pattipati, Y. Bar-Shalom, "A Multisensor-Multitarget Data Association Algorithm for Heterogeneous Sensors". *IEEE Trans on AES*, 29 (2): 560-568, 1993.

[2] Deb S., M. Yeddanapudi, K. Pattipati, Y. Bar-Shalom, "A Generalised S-D Assignment Algorithm for Multisensor-Multitarget State Estimation". *IEEE Trans on AES*, 33 (2): 523-536, 1997.

[3] Hough P.V.C., Method and means for recognising complex patterns, U.S. Patent 3,069,654. Dec. 1962.

[4] Blackman SS, *Multiple-Target Tracking with Radar Applications.* Artech House, 1986.